Analysis of Local Wind Circulation in Summer over the Kanto Plain Using the Adjustment Technique of Observed Wind with Roughness Parameter

Takahashi, Hideo / SETO, Yoshihito

(出版者 / Publisher)
Japan Climatology Seminar
(雑誌名 / Journal or Publication Title)
Japanese progress in climatology / Japanese progress in climatology
(巻 / Volume)
2011
(開始ページ / Start Page)
1
(終了ページ / End Page)
10
(発行年 / Year)
2011-12

Geographical Review of Japan Series A 84–6 529–552 2011

Analysis of Local Wind Circulation in Summer over the Kanto Plain Using the Adjustment Technique of Observed Wind with Roughness Parameter

SETO Yoshihito* and TAKAHASHI Hideo**

(* Graduate Student, Tokyo Metropolitan University, ** Tokyo Metropolitan University)

This study clarifies the vertical structure of diurnal variation in local wind systems, including sea breezes over the Kanto region, by focusing on temporal changes in the wind system structure caused by large-scale sea-breeze development. Because direct observation of the atmosphere's vertical motion is difficult, we developed an alternative index in which the quantity of divergence is calculated using observed surface wind data. However, observed surface wind data are inappropriate for calculating divergence fields because of differences in the observation heights of wind at different stations. Therefore, a roughness parameter corresponding to the wind direction at each observation point is estimated from land utilization data around the observation points based on the empirical formula proposed by Kuwagata and Kondo (1990). The adjustment of wind velocity is based on the logarithmic law of wind velocity. After adjustment, the wind velocity in the area near Tokyo Bay and absolute values of the quantity of divergence increased.

Typical sea-breeze days were selected, and temporal changes in the characteristics of the average wind and divergence fields were examined. Next, correlation coefficients of the quantity of divergence were calculated between marked divergence areas and each grid point in the study area. This analysis was performed to understand the relationship between the divergence and convergence areas and to identify areas where the diurnal variation in the divergence value is equal to that of marked divergence areas. At 09:00, a divergence area formed in Tokyo Bay (area TB), and sea-breeze circulation was observed between area TB and the convergence area in the neighborhood of Tokyo. At 11:00, with sea-breeze development, the influence of the Sagami Bay sea breeze in area TB weakened the correlation with the convergence area of Tokyo. Conversely, a valley wind developed in North Kanto, and valley wind circulation was observed between the divergence area around the prefectural border between Gunma and Saitama (area GS) and the convergence area of a neighboring mountainous district. It appears that typical valley wind circulation developed on a comparatively small scale; moreover, at that time, the valley wind circulation of North Kanto appeared to be independent of the sea-breeze circulation of South Kanto. After midday, the original correlation level with area TB was observed in the area between Kanagawa and Sagami Bay, which suggested a switch from the typical sea-breeze circulation to a large-scale sea breeze. With this large-scale sea-breeze development, the valley wind circulation in North Kanto became indistinct. Simultaneously, area TB developed a negative correlation with area GS. When the large-scale sea-breeze development was marked, the divergence in area GS corresponding to valley wind circulation weakened.

Key words: local circulation, land-sea breeze, roughness parameter, logarithmic law, Kanto plain

Table 1 Description of data

観測機関	使用データ	地点数	風の観測間隔	風速計の設置高度	風向風速以外の主な観測要素
気象庁	地域気象観測（アメダス）	134	10 分	6～75 m（平均 10 m）	気温・日照時間・降水量
	気象官署	(27)	(10 分)	10～75 m（平均 20 m）	気圧・気温・湿度・日照時間・降水量
(株) ライフビジネスウェザー	L-Robo	29	10 分	6～30 m（平均 20 m）	気圧・気温・湿度・日射量・降水量
海上保安庁	沿岸海上気象データ (MICS)	12	30 分（毎時 25, 55 分）	3～55 m（平均 25 m）	気圧（6 地点）
		6	15 分		

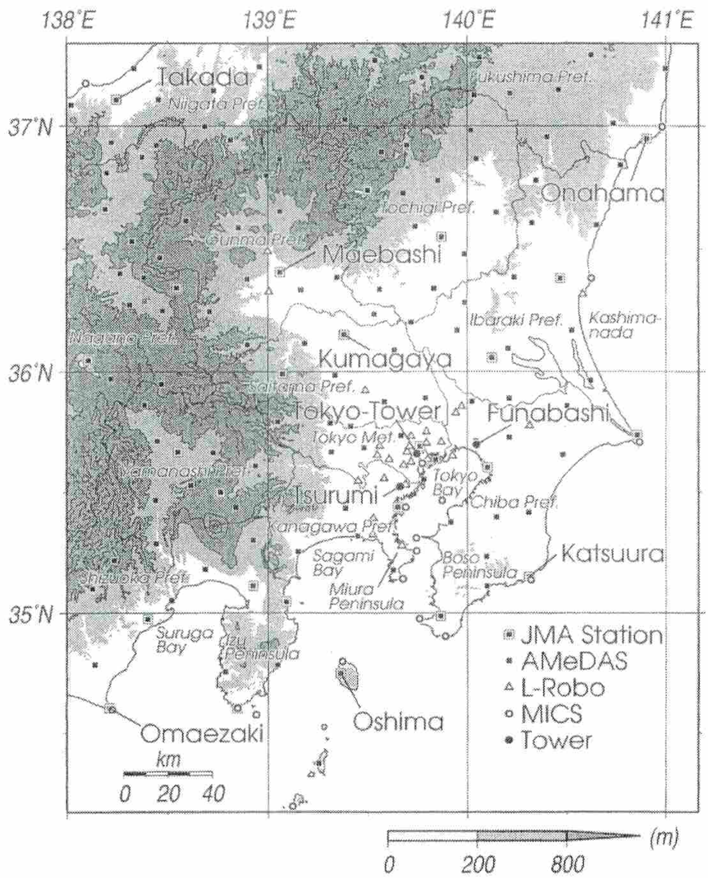

Fig. 1 Map of the study area showing distribution of observatories

Table 2　Land utilization divisions and classified categories

〈1976 年度〉土地利用種別	カテゴリー	〈1997 年度〉土地利用種別	カテゴリー
1　田※3	*a*	1　田※3	*a*
2　畑※3	*a*	2　その他の農用地※3	*b*
3　果樹園※4	*b*		
4　その他の樹木畑	*b*		
5　森林	*b*	5　森林	*c*
6　荒地※3	*a*	6　荒地※3	—
7　建物用地（大）	*c*	7　建物用地	*d*
8　建物用地（小）	*d*		
9　幹線交通用地	*a*	9　幹線交通用地	*e*
A　その他の用地※3	*a*	A　その他の用地※3	—
B　湖沼※1	*a*	B　河川地および湖沼※1	*a*
C　河川地 A※1	*a*		
D　河川地 B※3	*a*		
E　海浜※2	*a*	E　海浜※2	*b*
F　海水域※1	*a*	F　海水域※1	*a*
		G　ゴルフ場※3	*b*

※1：0.1 cm，※2：1 cm，※3：5 cm，※4：65 cm

Categories in 1976 were classified by Kuwagata and Kondo (1990).

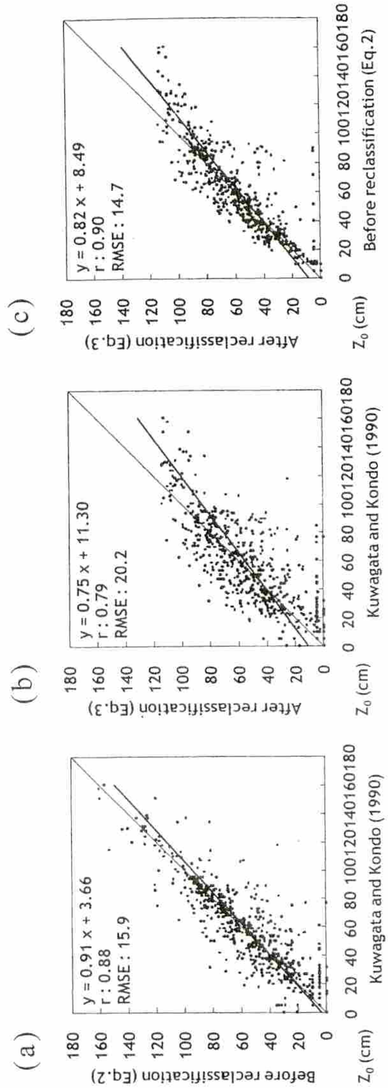

Fig. 2　Comparison of Z_0 estimated in this study and values in Kuwagata and Kondo (1990)

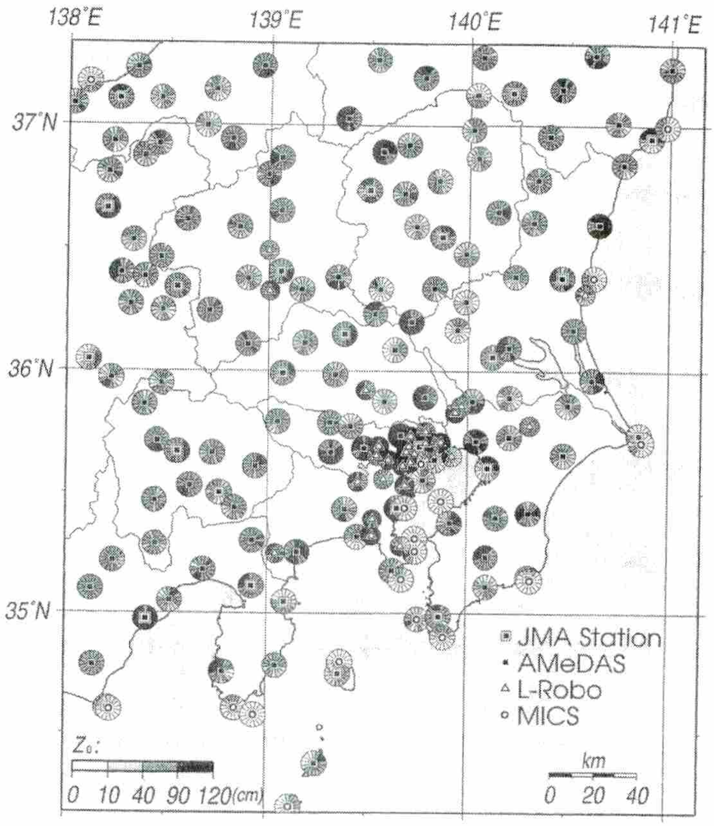

Fig. 3 Z_0 values at each observatory estimated in this study

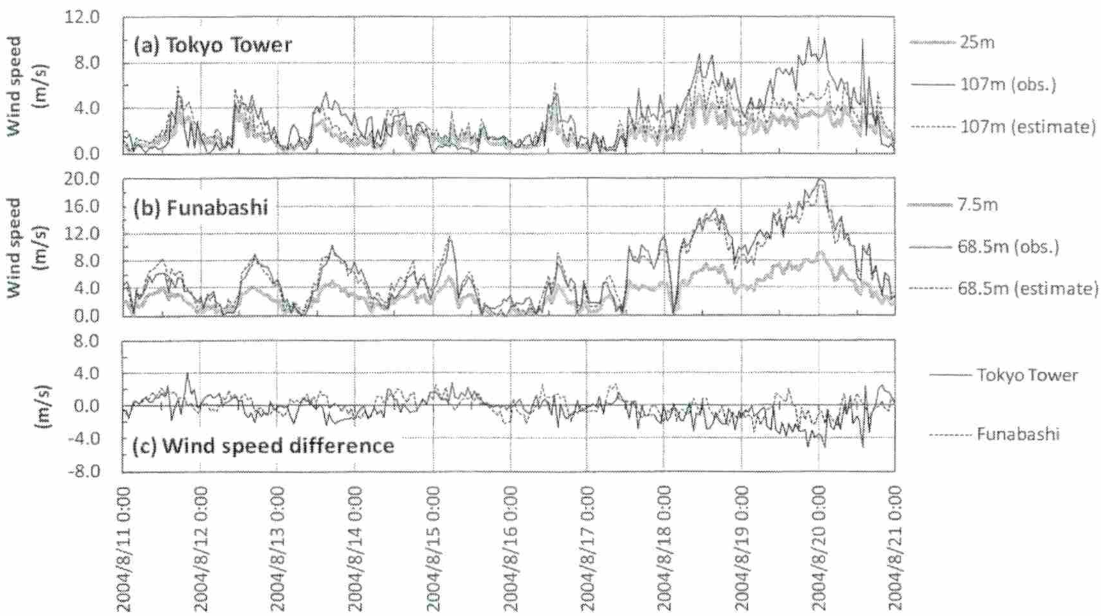

Fig. 4 Observed wind speed and estimated wind speed at tower stations in mid-August 2004

Table 3　Comparison of upper-layer wind speed from observations and those from estimations at tower stations

安定度		東京タワー（下層：25 m　上層：107 m）					船橋（下層：7.5 m　上層：68.5 m）				
		平均風速（m/s）		風速差（m/s）		事例数	平均風速（m/s）		風速差（m/s）		事例数
		観測値	推定値	平均値	RMSE		観測値	推定値	平均値	RMSE	
弱風時	全事例	1.7	1.6	−0.1	1.3	1,440	2.5	2.4	−0.1	0.9	697
	安　定	1.6	1.5	−0.1	1.3	922	2.6	2.0	−0.6	1.1	277
	中　立	1.8	1.7	−0.1	1.3	362	2.6	2.7	0.1	0.7	272
	不安定	1.9	1.9	0.0	1.3	156	1.9	2.7	0.7	0.9	148
強風時	全事例	4.6	4.3	−0.4	2.2	768	7.3	7.6	0.3	1.1	1,511
	安　定	5.0	4.1	−0.9	2.4	250	9.0	7.9	−1.0	1.3	189
	中　立	4.2	4.1	−0.1	2.0	237	6.9	6.8	−0.1	0.9	537
	不安定	4.6	4.5	−0.1	2.3	281	7.1	8.0	0.9	1.3	785

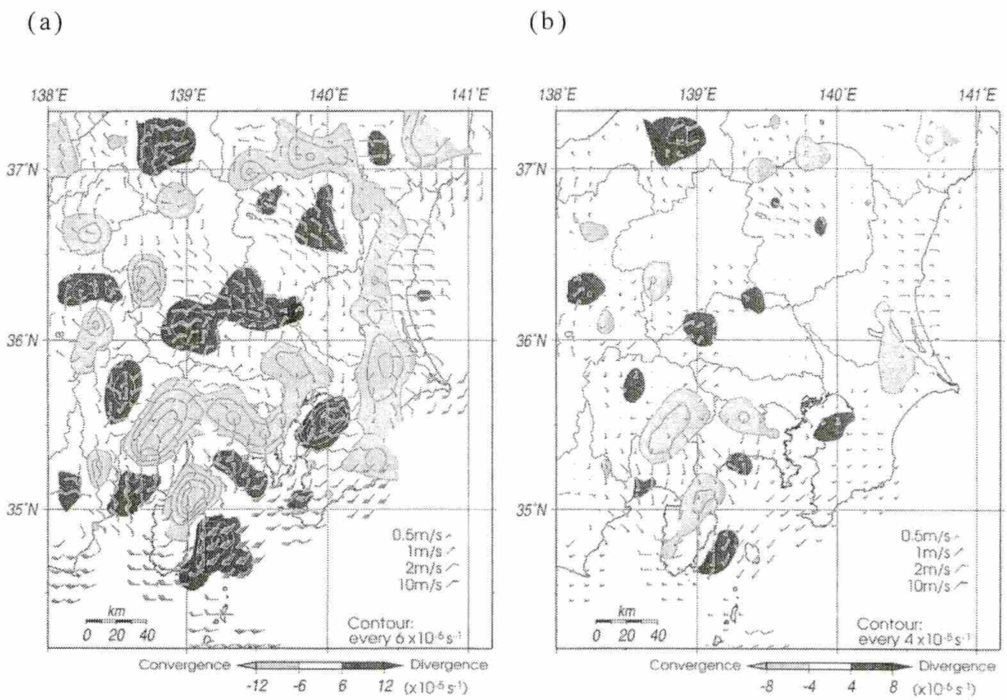

Fig. 5　Distribution maps showing wind barbs and divergence at 11:00 JST on August 13, 2004
(a) Adjustment applied; (b) deviation without adjustment.

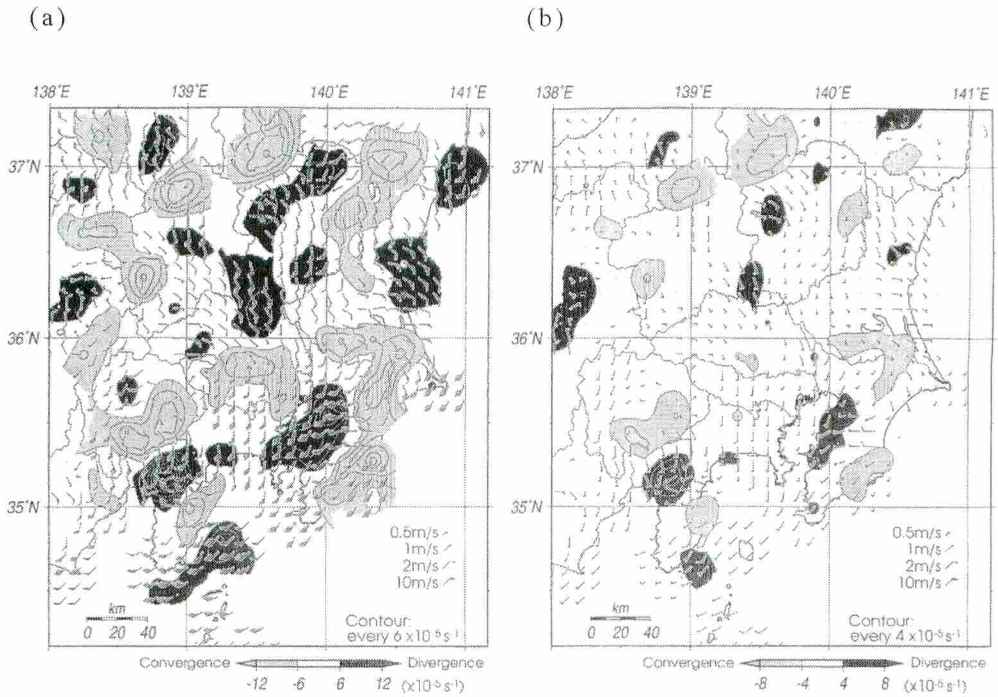

Fig. 6 Distribution maps showing wind barbs and divergence at 15:00 JST on August 13, 2004
(a) Adjustment applied; (b) deviation without adjustment.

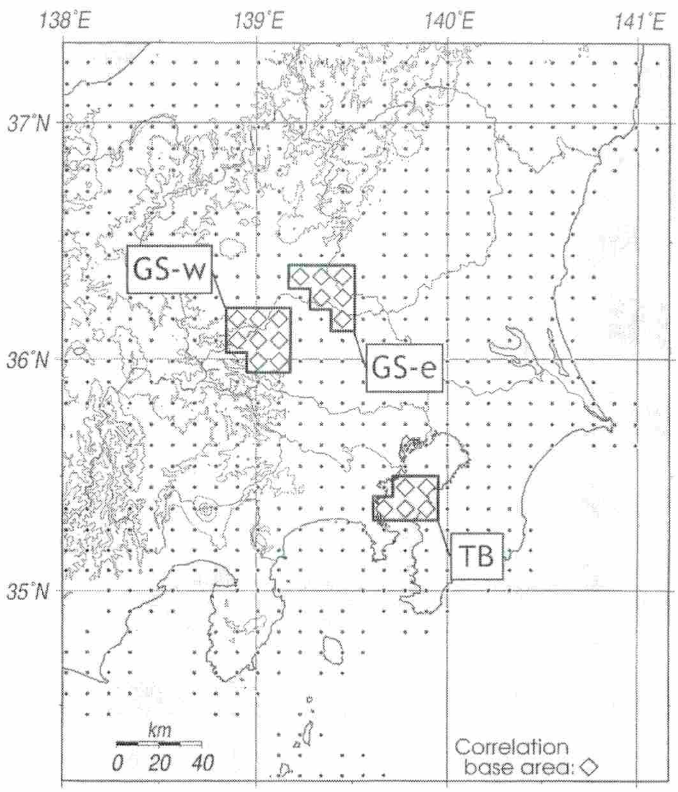

Fig. 8 Divergence areas used for standard correlation

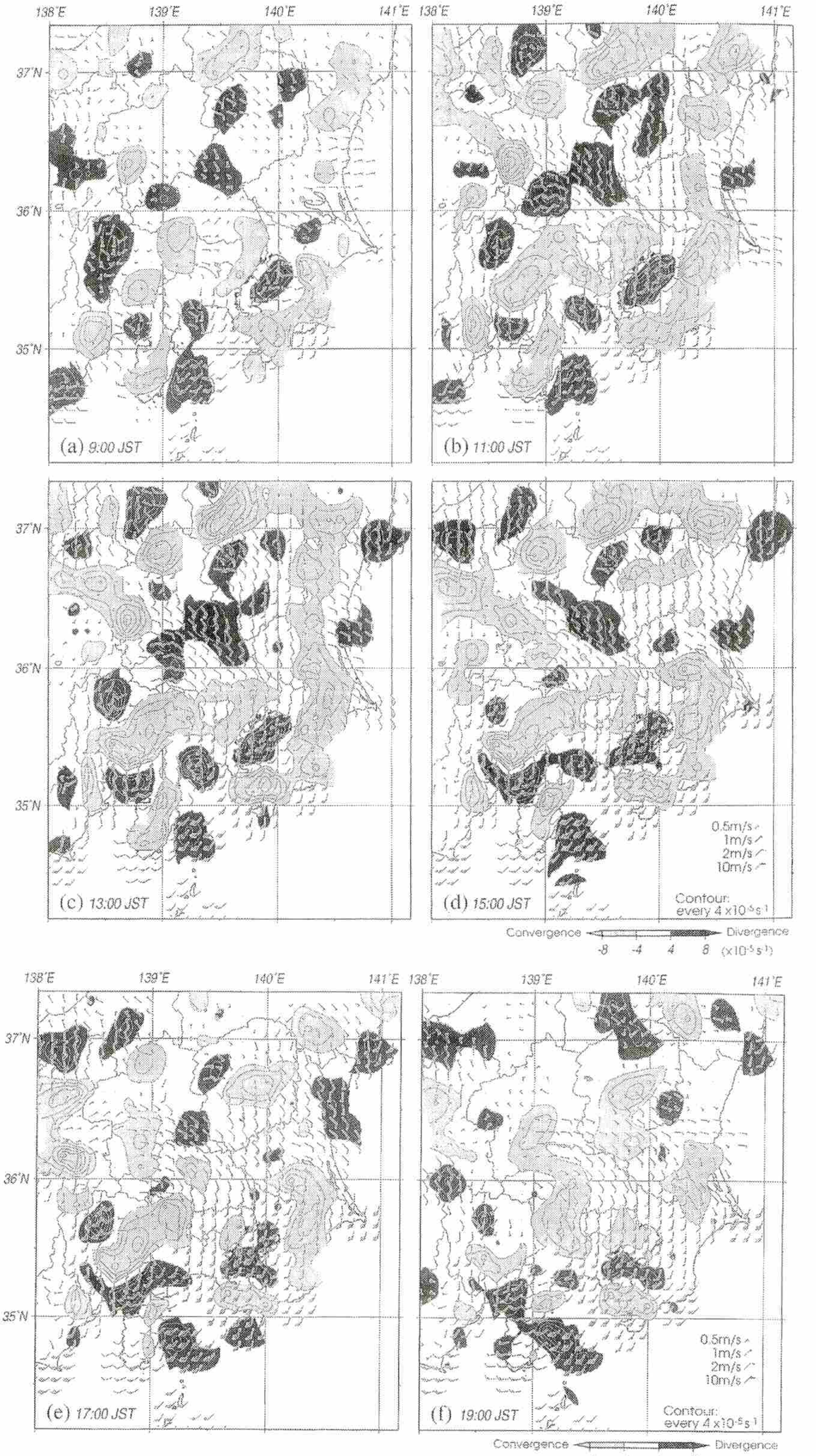

Fig. 7　Distribution maps showing composite wind barbs and divergence on 9 sea-breeze days
(a) 09:00 JST; (b) 11:00 JST; (c) 13:00 JST; (d) 15:00 JST; (e) 17:00 JST; (f) 19:00 JST.

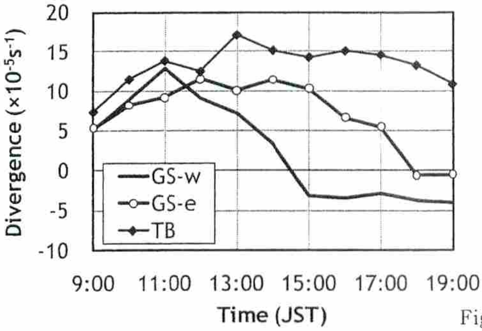

Fig. 9 Time series of the value of divergence in each divergence area

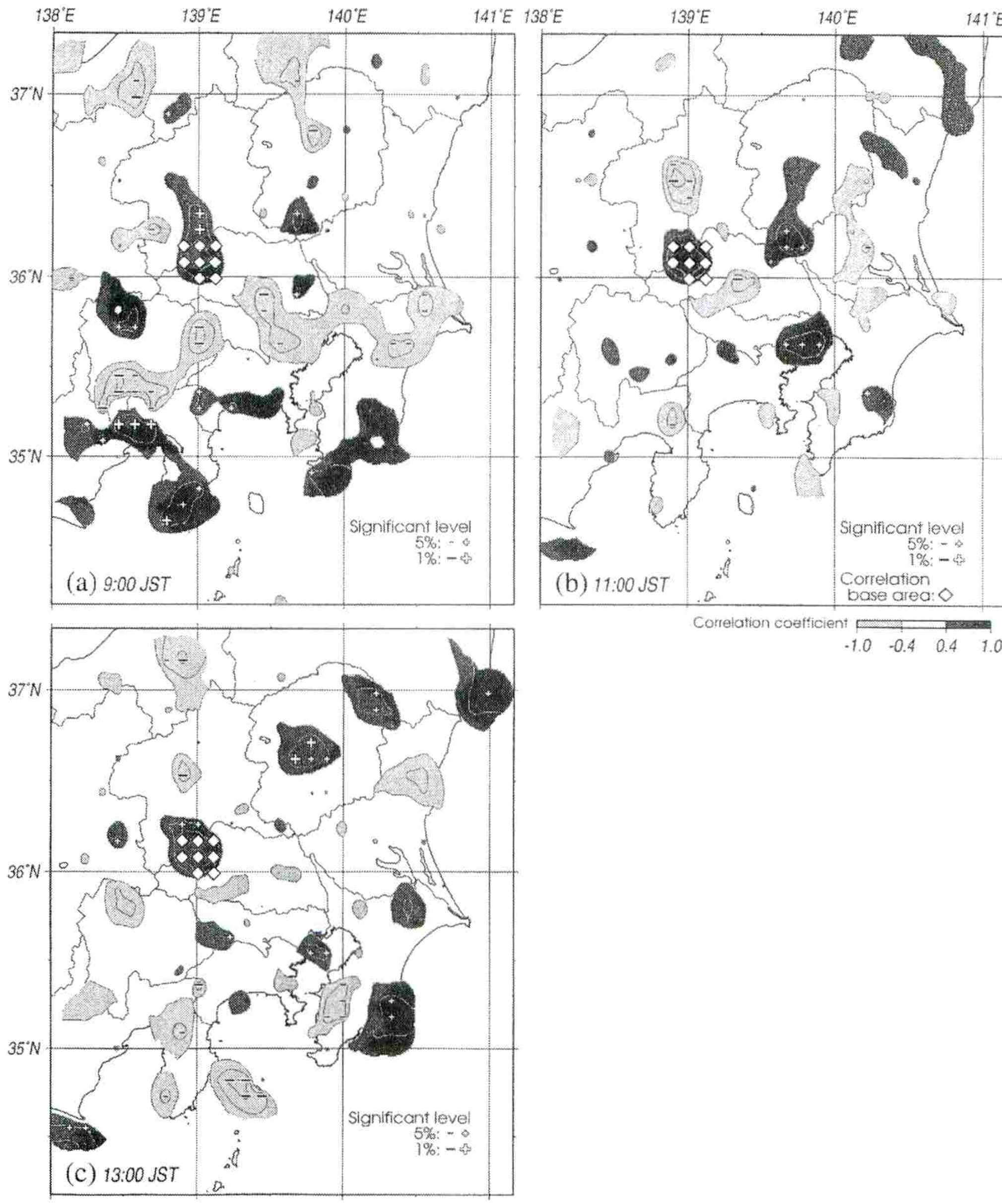

Fig. 10 Correlation with the value of divergence in area GS-w
(a) 09:00 JST; (b) 11:00 JST; (c) 13:00 JST.

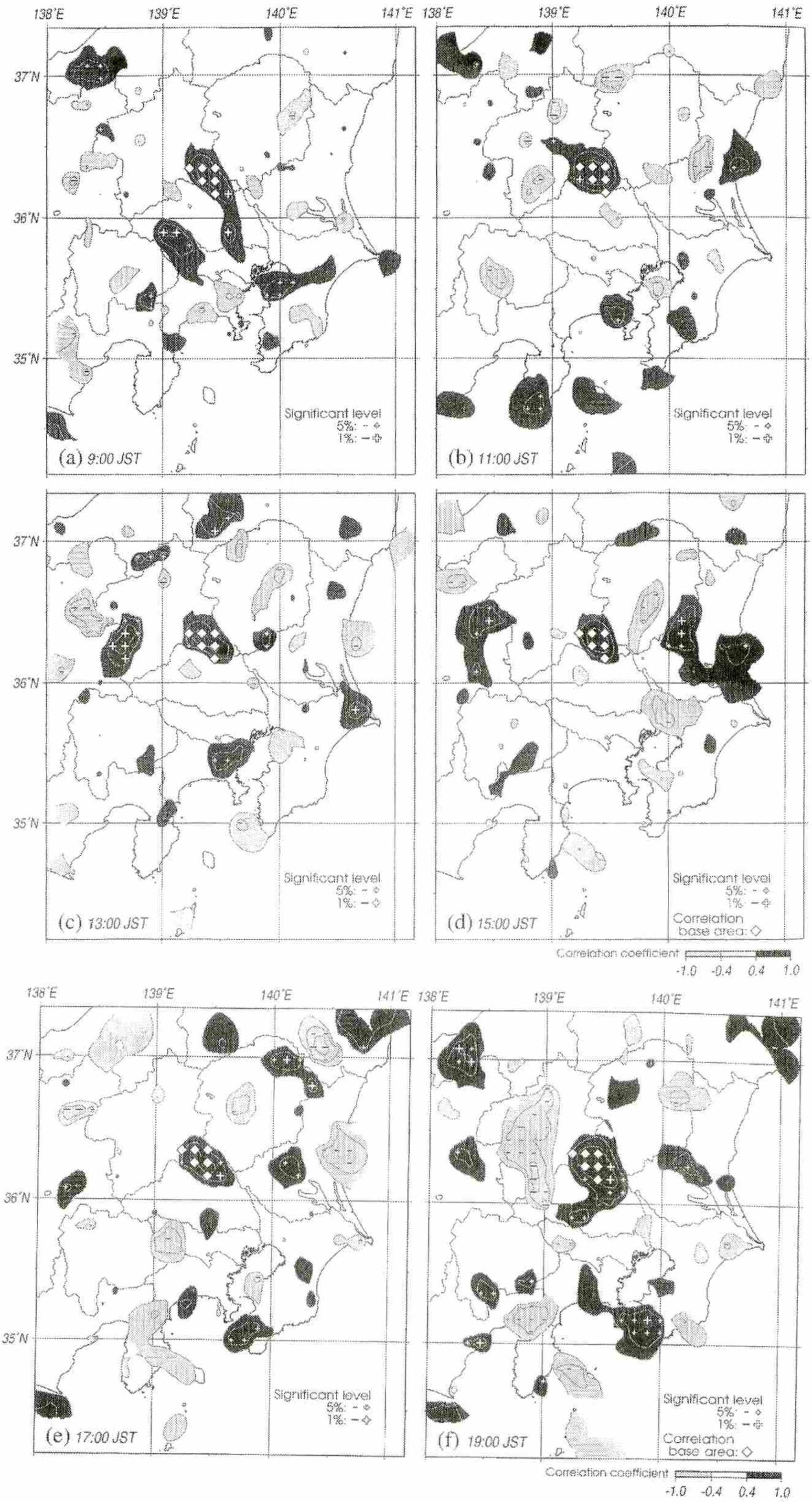

Fig. 11 Correlation with the value of divergence in area GS-e
(a) 09:00 JST; (b) 11:00 JST; (c) 13:00 JST; (d) 15:00 JST; (e) 17:00 JST; (f) 19:00 JST.

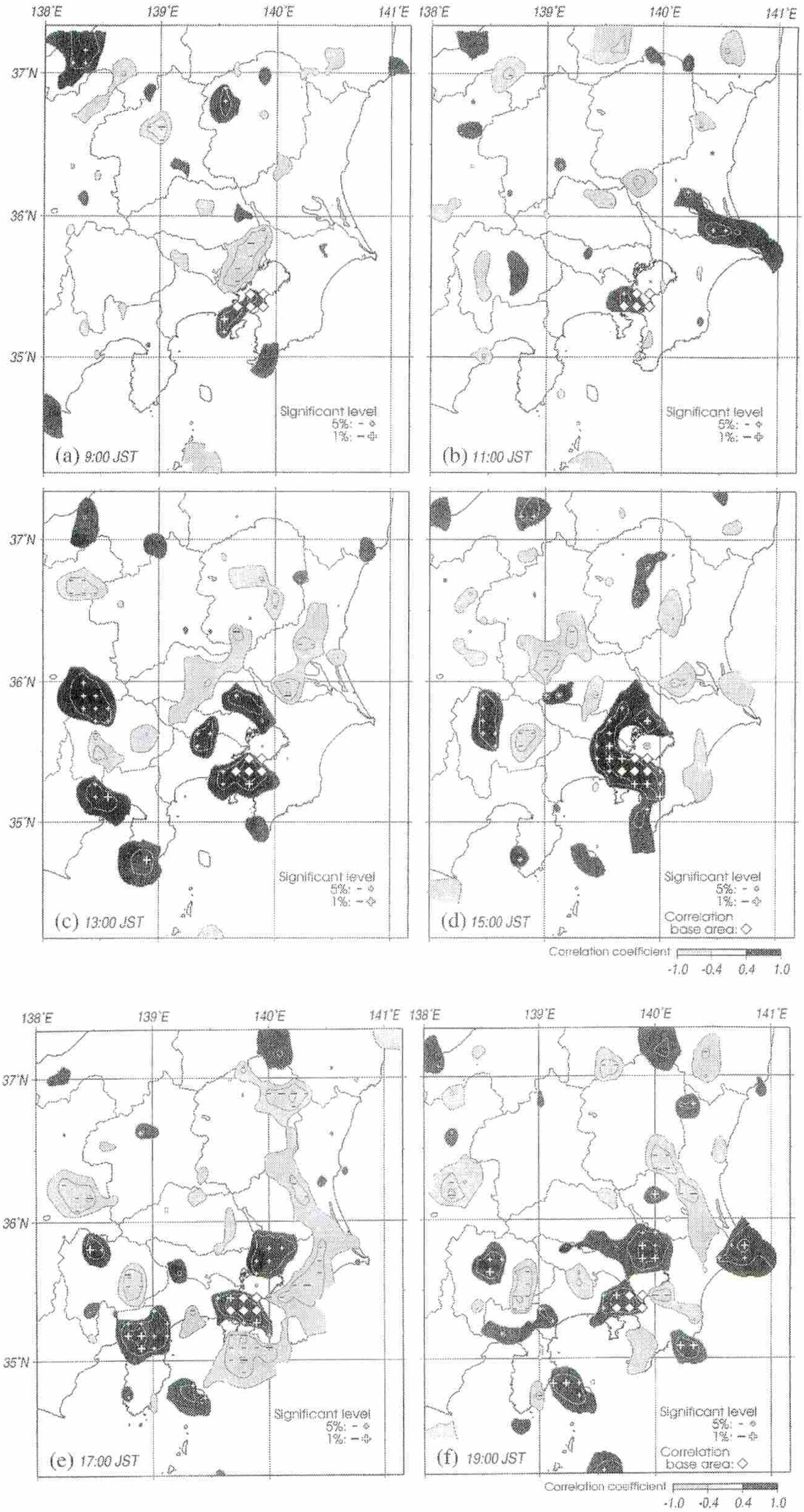

Fig. 12 Correlation with the value of divergence in area TB
(a) 09:00 JST; (b) 11:00 JST; (c) 13:00 JST; (d) 15:00 JST; (e) 17:00 JST; (f) 19:00 JST.